Theoretical predictions of vibration–rotation–tunneling dynamics of the weakly bound trimer H 2 O 2 HCl

ARTICLE *in* CHEMICAL PHYSICS LETTERS · AUGUST 2001

Impact Factor: 1.9 · DOI: 10.1016/S0009-2614(01)00754-0

4 AUTHORS, INCLUDING:

Tatiana Korona
University of Warsaw
66 PUBLICATIONS **1,528** CITATIONS

10 August 2001

ELSEVIER

Chemical Physics Letters 343 (2001) 588–596

CHEMICAL PHYSICS LETTERS

www.elsevier.com/locate/cplett

Theoretical predictions of vibration–rotation–tunneling dynamics of the weakly bound trimer $(H_2O)_2HCl$

Cezary Struniewicz [a], Tatiana Korona [a], Robert Moszynski [a,*], Anne Milet [a,b]

[a] *Department of Chemistry, University of Warsaw, Pasteura 1, 02-093 Warsaw, Poland*
[b] *Laboratoire d'Etudes Dynamiques et Structurales de la Sélectivité, UMR 5616, LEDSS VII, Chimie Théorique, Université Joseph Fourier, D.U. BP 53, 38041 Grenoble Cedex 9, France*

Received 16 May 2001; in final form 13 June 2001

Abstract

In this Letter we report a theoretical study of the vibration–rotation–tunneling (VRT) states of the $(H_2O)_2HCl$ trimer. Five degrees of freedom are considered: two angles corresponding to the torsional (flipping) motions of the free, non-hydrogen-bonded, hydrogen atoms in the complex, and three angles describing the overall rotation of the trimer in the space. A two-dimensional potential energy surface is generated ab initio by symmetry-adapted perturbation theory (SAPT). Tunneling splittings, frequencies of the intermolecular vibrations, and vibrational line strengths of spectroscopic transitions are predicted.

1. Introduction

Molecular complexes containing water molecule are the subject of continuing investigations in the fields of atmospheric chemistry, catalytic reactions, surface chemistry, and biological processes. The study of the interaction between water and hydrogen chloride is of fundamental importance for the understanding of the production of stratospheric chlorine molecules which, in turn, take part in the catalytic ozone depletion reactions. The mainly heterogeneous atmospheric reaction beginning with the adsorption of the HCl molecules on the surface of water icicles is the source of the stratospheric chlorine atoms in the polar regions [1–3]. Chlorine molecules are photolyzed by solar radiation and the resultant chlorine atoms take part in the destruction of the stratospheric ozone. The study of the $(H_2O)_nHCl$ clusters is an important step towards understanding of the behavior of the HCl molecule on the ice surface [4–7].

Only the first members of the $(H_2O)_nHCl$ series have been observed by means of high-resolution spectroscopy. The rotational spectrum of the dimer H_2OHCl has been first recorded and analyzed by Legon et al. [8], and reinvestigated by Kisiel and collaborators [9]. Recently, Kisiel et al. [10,11] reported the observation of the second member of the series, $(H_2O)_2HCl$, also by rotational spectroscopy.

The theoretical determination of the structure of the $(H_2O)_2HCl$ trimer was first presented in [12]. In a recent series of papers [13,14] we reported a detailed theoretical investigations of $(H_2O)_2HCl$, and compared our theoretical predictions with the

* Corresponding author.
E-mail address: rmoszyns@chem.uw.edu.pl (R. Moszynski).

0009-2614/01/$ - see front matter
PII: S0009-2614(01)00754-0

experimental results from the rotational spectroscopy [10,11]. The structure, molecular properties, and the qualitative picture of the vibration–rotation–tunneling (VRT) dynamics were in excellent agreement with the experimental data [10,11]. In this Letter we report quantitative predictions of the VRT motions in the complex. First we compute the potential energy surface for the flipping motions of the non-hydrogen-bonded hydrogens in the $(H_2O)_2HCl$ trimer, and next present calculations of the VRT states, transition frequencies, and the corresponding line strengths.

2. Methods of calculations

2.1. Potential energy surface

The potential energy surface for the flipping dynamics of the hydrogens in the $(H_2O)_2HCl$ trimer was computed by symmetry-adapted perturbation theory (SAPT):

$$E_{\text{int}}^{\text{SAPT}} = E_{\text{int}}^{\text{SAPT}}(2,3) + E_{\text{int}}^{\text{SAPT}}(3,3). \tag{1}$$

The pair interaction energy, $E_{\text{int}}^{\text{SAPT}}(2,3)$ was computed from the following expression:

$$E_{\text{int}}^{\text{SAPT}}(2,3) = E_{\text{elst}}^{(1)} + E_{\text{ind}}^{(2)} + E_{\text{disp}}^{(2)} + E_{\text{exch}}, \tag{2}$$

where the consecutive terms on the RHS of Eq. (2) denote the electrostatic, induction, dispersion, and exchange energies, respectively, and have been evaluated using the many-body techniques developed in [15–23]. The exchange-deformation energy was computed directly from the supermolecule Hartree–Fock interaction energy. The computational scheme for the pair interactions was the same as in [13,14] (see also [24] for a review). The SAPT calculations of the pair interaction energies were made with the program SAPT [25]. The pair energies were always computed with dimer basis sets.

The non-additive part of the interaction energy, $E_{\text{int}}^{\text{SAPT}}(3,3)$, was given by:

$$E_{\text{int}}^{\text{SAPT}}(3,3) = E_{\text{ind,resp}}^{(2)} + E_{\text{ind,resp}}^{(3)} + E_{\text{ind–disp,RPA}}^{(3)} + E_{\text{disp,RPA}}^{(3)} + E_{\text{exch}}, \tag{3}$$

where $E_{\text{ind,resp}}^{(2)}$ and $E_{\text{ind,resp}}^{(3)}$ denote the second- and third-order non-additive induction energies accounting for the orbital relaxation, $E_{\text{ind–disp,RPA}}^{(3)}$ and $E_{\text{disp,RPA}}^{(3)}$ are the third-order induction–dispersion and dispersion non-additivities, and E_{exch} denotes the total non-additive exchange contribution. The subscript "RPA" at $E_{\text{ind–disp,RPA}}^{(3)}$ and $E_{\text{disp,RPA}}^{(3)}$ means that in the calculations of these contributions the response functions of the random-phase approximation (RPA) were employed. See [26,27] for the theoretical bases of Eq. (3), and [27,28] for the computational details. All calculations of the three-body energies were done with the SAPT3 system of codes [29]. The full basis of the trimer was used in these calculations.

2.2. Rovirational Hamiltonian

As shown in [13] the group of feasible permutation–inversion operations [30] for the $(H_2O)_2HCl$ complex is $G_8 = \{E, E^\star\} \otimes \{E, (12), (34), (12)(34)\}$. Thus, the VRT states of the complex can be classified according to the irreducible representations (irreps) of this group. It was also shown [13] that the flipping motions in the complex are governed by the inversion operation $E^\star$, while other tunneling motions are governed by the PI operations $(12)^\star$ and $(34)^\star$. Since the flipping barriers separating the equivalent minima are low [13], one can expect that the VRT levels can, in the first approximation, be classified according to the $A^\pm$ irreps of G_2.

In this Letter we consider the simplest model of the trimer dynamics corresponding to low-energy tunneling motions, i.e. to the hydrogen flipping in the trimer. All coordinates except for the flipping angles are frozen. In particular, the bond lengths r(O–H) in H_2O and r(H–Cl) in HCl were fixed at their experimental values [10]. If we restrict the internal motions in the trimer to the flipping motions the Hamiltonian for the nuclear motion is given by:

$$H = H_{\text{int}} + H_{\text{asym}} + H_{\text{Cor}}, \tag{4}$$

where the consecutive terms on the RHS denote Hamiltonians describing the internal motions, the external rotational part given by the asymmetric top Hamiltonian, and the Coriolis term coupling

the internal motions with the overall rotations of the complex. The asymmetric rotor Hamiltonian is given by the standard expression:

$$H_{\text{asym}} = AJ_z^2 + BJ_x^2 + CJ_y^2, \tag{5}$$

where A, B, and C are the rotational constants of the trimer taken from the experimental paper of Kisiel et al. [10], and J_i, $i = x, y, z$, denote the components of the total angular momentum operator. We follow [31] and represent the internal Hamiltonian by the kinetic energy term describing the flipping motions in the complex, H_{flip}, and the potential V, $H_{\text{int}} = H_{\text{flip}} + V$. The Hamiltonian H_{flip} depends exclusively on the coordinates of the complex that define the flipping motion, i.e., on the set of two torsional angles (χ_1, χ_2). For the $(H_2O)_2HCl$ case H_{flip} and H_{Cor} are given by Eqs. (2) and (3) of [31], except that in our case the summations over v are restricted to two rather than to three water molecules.

The line strength of a transition from an initial level i to a final level f is given by:

$$S(i \to f) = \sum_m |\langle \Psi_f | \mu_m | \Psi_i \rangle|^2, \tag{6}$$

where Ψ_i and Ψ_f denote the wavefunctions of the initial and final states, respectively, and μ_m is the mth spherical component of the dipole moment of the complex with respect to the trimer frame. In our calculation the dipole function was represented by the sum of the permanent dipole moments of the monomers, i.e. the dipole function neglects the interaction between the monomers. Although this approximation was shown to be quite crude for the $(H_2O)_2HCl$ trimer [11], we believe that our results for the line strengths will be qualitatively correct.

2.3. Computational details

The potential for the flipping motions was computed as a function of the rotation angles χ_v, $v = 1, 2$, around the axes defined by the vectors connecting the hydrogen-bonded hydrogen atoms and the centers-of-mass of the water molecules, cf. Fig. 1. The angles χ_v vary from $-180°$ to $+180°$. However, for $\chi_v < -110°$ and $\chi_v > +110°$ the potential becomes repulsive, and does not contribute to the rovibrational levels of the complex. Thus, in actual calculations we restricted the domain of χ_v to $[-110°, +110°]$, and computed 60 points in (χ_1, χ_2) on this interval. In all calculations we employed the aug-cc-pVDZ basis [32]. The computed points are available from the authors on request.

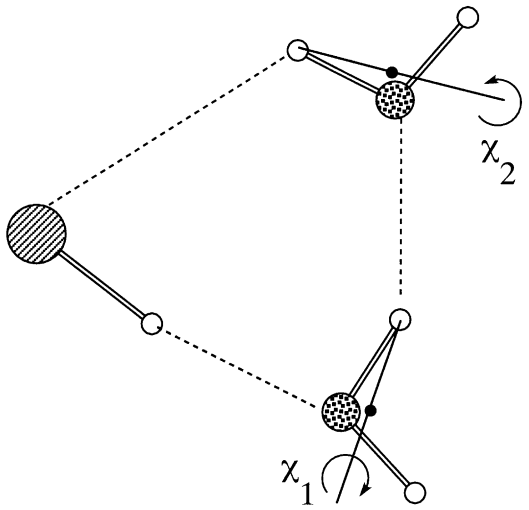

Fig. 1. Schematic definition of the rotation angles χ_1 and χ_2 for the flipping motions in the $(H_2O)_2HCl$ trimer.

It should be noted that the rovibrational Hamiltonian described above was derived for specific motions in the trimer such that the centers-of-mass of the water molecules, the hydrogen atoms forming hydrogen bonds, and the chlorine atom are fixed in one plane, and only the OH groups formed by the H atoms not involved in the hydrogen-bonding perform the flipping motions. This means that in the calculations of the potential energy surface in (χ_1, χ_2) the geometries of the trimer must fulfill the planarity constraint discussed above. The equilibrium structure of $(H_2O)_2HCl$ as computed by ab initio methods [12,13] or determined from the microwave spectra [10] shows small deviations from the planarity requirement. Therefore, in our calculations of the potential energy surface, the starting geometry for the variation of the angles χ_1 and χ_2 was represented by a slightly modified version [33] of the experimental equilibrium geometry of the trimer [10]. This modified equilibrium geometry was fitted

to reproduce the experimental rotational constants [10] with the planarity constraint discussed above. The rotational constants corresponding to this geometry differ by less than 0.02% from the experimental rotational constants, so the latter can be used in the dynamical calculations of the rovibrational levels.

The computed points on the potential surface were fitted to the following expression:

$$V(\chi_1,\chi_2)=\sum_{i,j=0}^{i+j=4} c_{ij}\chi_1^i\chi_2^j, \tag{7}$$

with c_{ij} serving as adjustable parameters. Given the symmetry of the potential, $V(\chi_1,\chi_2)=V(-\chi_1,-\chi_2)$, resulting directly from the G_2 permutation–inversion symmetry considered above, only terms with even $i+j$ appear in Eq. (7). The coefficients c_{ij} were obtained from a straightforward linear least-square fit without any weighting factors. The fitted function reproduced the computed points within 1% or better. The parameters of the fit are available from the authors on request. A similar expression has been used to fit the two-body potential alone.

The manifolds of the VRT states for $J=0$ and $J=1$ were obtained by diagonalizing the internal Hamiltonian $H_{\rm int}$ in the discrete variable representation. The corresponding basis set consisted of products of two sine functions of χ_1 and χ_2, respectively [34]. A grid limited to $-110^\circ\leqslant\chi_v\leqslant+110^\circ$ was used with a spacing of 10°. We have checked that with this grid spacing and boundaries the first few eigenvalues are converged to within 0.1 cm^{-1} or better. Since no experimental data are available yet, we decided not to put any extra computational effort to get better convergence of the results. For $J=1$ the internal basis was multiplied by the symmetric rotor functions $[(2J+1)/8\pi^2]^{1/2}\mathscr{D}^{(J)\star}_{MK}(\alpha,\beta,\gamma)$. In the latter case the J and M quantum numbers were fixed and K was mixed by asymmetric rotor Hamiltonian, $H_{\rm asym}$, and by the Coriolis coupling of the internal motions with the overall rotations, $H_{\rm Cor}$. In order to judge the effect of the three-body interactions on the VRT levels and tunneling splittings, we performed the dynamical calculations with the total SAPT potential, and with the pair potential alone.

3. Theoretical predictions

3.1. Features of the potential energy surface

The computed potential reveals two equivalent global minima of -3866.03 cm^{-1} for $(\chi_1,\chi_2)=(-56^\circ,23^\circ)$ and $(\chi_1,\chi_2)=(56^\circ,-23^\circ)$. These two minima are separated by a barrier of 196.0 cm^{-1}. The corresponding saddle point is located at $(\chi_1,\chi_2)=(0^\circ,0^\circ)$. See Fig. 2a for the contour plot of the SAPT potential.

It is worth noting that the three-body forces contribute significantly to the well depth of the potential. The minimum of the two-body potential is located around $(\chi_1,\chi_2)=(-50^\circ,20^\circ)$, and its depth is -3368.1 cm^{-1}, i.e. ≈15% higher than the depth of the total SAPT potential. Surprisingly, the corresponding change is the barrier is less pronounced. The height computed from the two-body potential alone amounts to 211.7 cm^{-1}, and is 8% higher than the barrier of the total, pair plus three-body, potential.

The contour plots of the SAPT pair and three-body potentials are reported in Figs. 2b and c, respectively. Comparison of Figs. 2a and b shows that the anisotropy of the total potential closely follows the pair anisotropy. Only at small angles, substantial differences can be observed. Here, the pair potential shows a more pronounced angular dependence. The three-body potential is almost symmetric with respect to separate changes $\chi_1\to-\chi_1$ or $\chi_2\to-\chi_2$, cf. Fig. 2c. This approximate symmetry of the non-additive potential cannot be attributed to a single energy contribution, cf. Eq. (3). We have checked that the two major components of the non-additive three-body potential, i.e. the second-order induction non-additivity, $E^{(2)}_{\rm ind,resp}$, and the exchange three-body contribution, $E_{\rm exch}$, show a similar angular dependence.

As shown in [13,14] the SAPT pair and three-body energies are in a quantitative agreement with the results of supermolecule coupled-cluster calculations including single, double, and non-iterative triple excitations. This quantitative agreement held for various geometries of the trimer, so our potential energy surface is expected to be rather accurate.

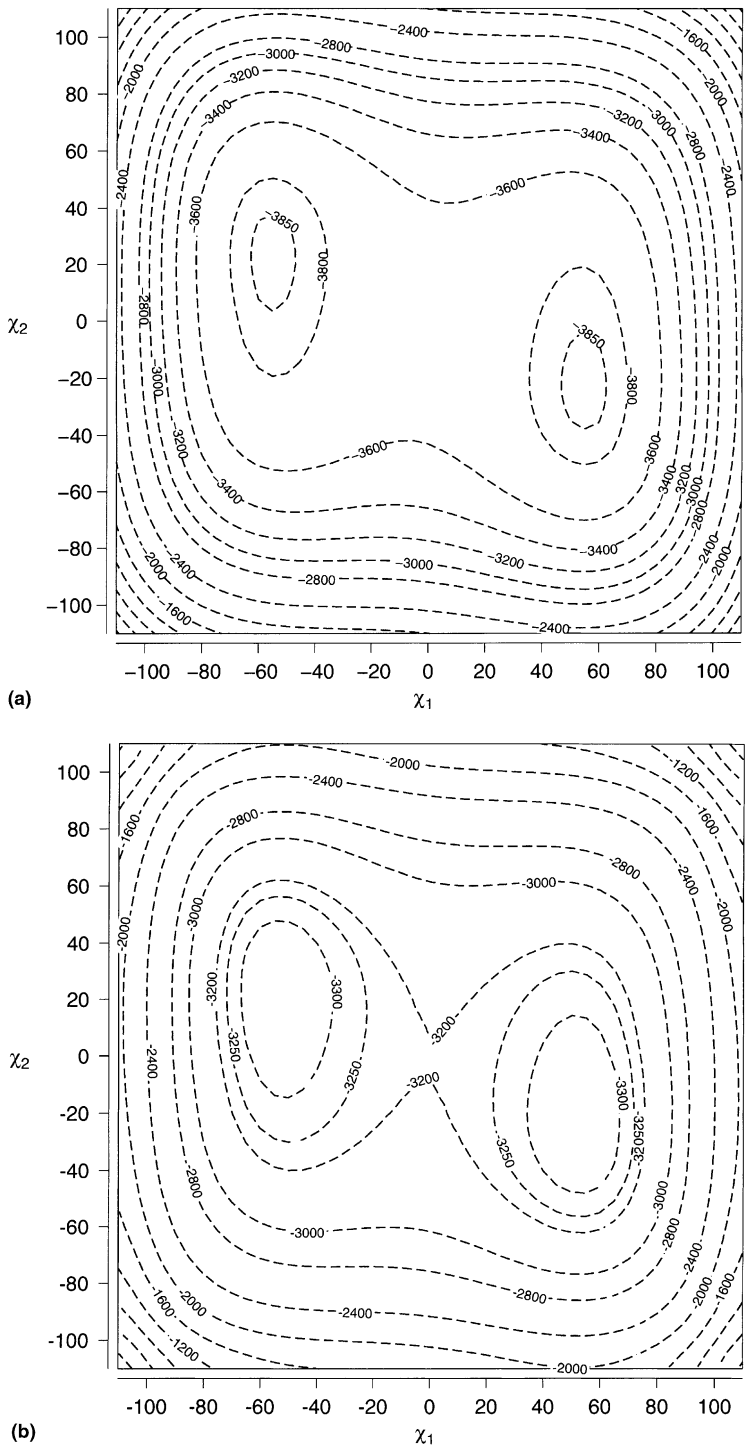

Fig. 2. Contour plots (in cm^{-1}) of the (a) total, (b) pair, and (c) three-body SAPT potential energy surfaces for the flipping motions in the $(H_2O)_2HCl$ trimer.

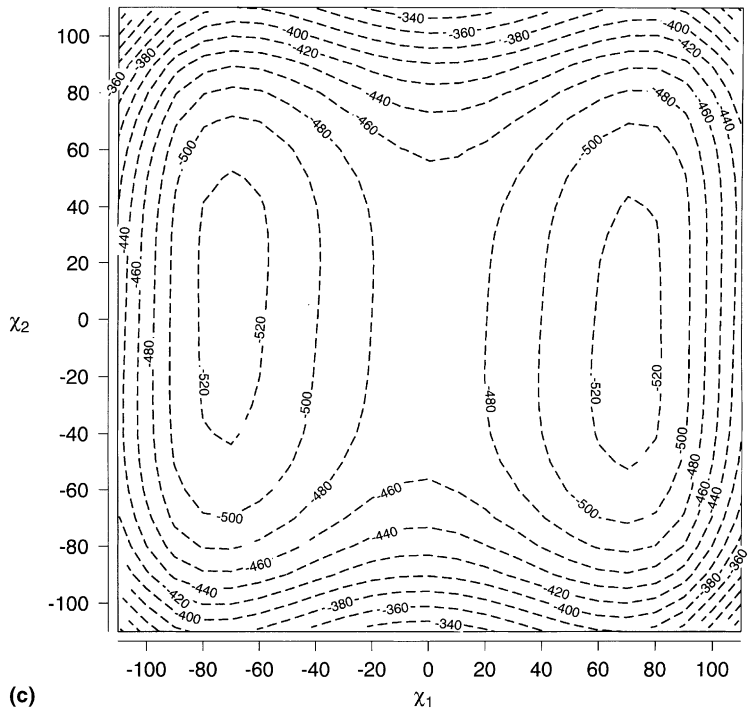

Fig. 2. *(Continued)*.

3.2. Vibration–rotation–tunneling dynamics

The energies of the ten lowest states for $J = 0$ and $J = 1$ are reported in Table 1. The energy of the zero-point vibration is $D_0 - D_e = 169.69\ \mathrm{cm}^{-1}$. An inspection of Table 1 shows that the energy levels for $J = 0$ are grouped into pairs of states of A^+ and A^- symmetry, separated by small energy

Table 1
Lowest rovibrational energy levels for $J = 0$ and $J = 1$. The energy levels are given in cm^{-1} with respect to the ground state. For $J = 0$ the values computed from the total and pair SAPT potentials are reported. For $J = 1$ the energy levels were generated from the total SAPT potential with the Coriolis term neglected ($E_{\mathrm{no-Cor}}$) and included (E_{exact})

	$J = 0$			$J = 1$		
		E_i			E_i	
i	Symmetry	Total	Pair	Symmetry	$E_{\mathrm{no-Cor}}$	E_{exact}
1	A^+	0.00	0.00	A^+	0.179 (1_{01})	0.176
2	A^-	19.33	27.65	A^-	0.302 (1_{11})	0.299
3	A^-	130.30	126.52	A^-	0.335 (1_{10})	0.329
4	A^+	139.44	139.80	A^-	19.510 (1_{01})	19.506
5	A^+	177.02	177.15	A^+	19.631 (1_{11})	19.629
6	A^-	263.80	259.70	A^+	19.665 (1_{10})	19.660
7	A^+	281.24	272.85	A^-	130.480 (1_{01})	130.479
8	A^-	292.31	293.27	A^+	130.602 (1_{11})	130.600
9	A^-	327.72	327.51	A^+	130.635 (1_{10})	130.631
10	A^+	391.86	388.18	A^+	139.619 (1_{01})	139.614

gaps. The energy difference of the two closest $A^{\pm}$ states is due to the tunneling, and is called the tunneling splitting. The magnitude of this splitting varies from a few wave numbers to almost one hundred. The lowest tunneling state, i.e. the first state of A^- symmetry, is located 19.33 cm^{-1} above the ground state, the second one is 9.14 cm^{-1} lower than the first excited state of A^+ symmetry, while the third one is 86.78 cm^{-1} above the second excited A^+ state.

Also reported in Table 1 are the $J = 0$ energy levels computed from the pair potential. The three-body interactions strongly affect the tunneling splittings of some states. The first two tunneling splittings are overestimated by as much as ≈43%, and the fourth one is overestimated by almost a factor of two. Surprisingly, the splittings of the second and fifth excited states are underestimated by only ≈5%.

The pattern of the levels is different for $J = 1$. If we neglect the Coriolis term in the Hamiltonian (4), the energy of each $J = 1$ state can be represented as:

$$E_{\text{no-Cor}} = E_{\text{flip}} + E_{\text{rot}}, \tag{8}$$

where E_{flip} and E_{rot} are the eigenvalues of H_{int} for $J = 0$ and H_{asym} for $J = 1$, respectively. Since the $(H_2O)_2HCl$ trimer is close to the oblate symmetric rotor limit (the rotational constants B and C are close), the states can be labeled with the conventional rigid rotor quantum numbers $J_{K_aK_c}$ with $K \equiv K_a$. In our case the labels of the three lowest $J = 1$ states are 1_{01}, 1_{11}, and 1_{10}, and these three labels will describe the rotational part of the wavefunctions for the consecutive triples of states. The symmetry labels of the rovibrational wavefunctions for $J = 1$ follow from the fact that the 1_{01}, 1_{11}, and 1_{10} rigid rotor states are of A^+, A^-, and A^- symmetry, respectively. When the Coriolis interaction is switched on the energy levels can no longer be represented by Eq. (8). However, an inspection of Table 1 shows that the Coriolis coupling of the internal motions with the overall rotation of the trimer is negligibly small. Comparison of the exact eigenvalues of the total Hamiltonian (4), denoted in Table 1 by E_{exact}, with the levels computed from Eq. (8) gives us the magnitude of the Coriolis coupling for $J = 1$. For all the states considered in Table 1 the difference $E_{\text{exact}} - E_{\text{no-Cor}}$ is very small, of the order of 10^{-3} cm^{-1}, and can be neglected in the first approximation.

For $J \neq 0$ the tunneling splitted counterparts of the states of A^+ symmetry should be described by the same rotational wavefunction, i.e. the rigid rotor label $J_{K_aK_c}$ for the tunnel splitted state A^- should be the same as for A^+. Given the fact that the rotational spacings are very small, and that the Coriolis interaction is negligible, the pattern of the splittings is almost the same as for $J = 0$, except that now we observe the tunneling splittings grouped into triples very close in energy. Within one triple the corresponding energy differences in the splittings are exclusively caused by the Coriolis interaction, and thus are very small. Still, they could be observed in a high-resolution experiment.

The far-infrared spectrum of the $(H_2O)_2HCl$ trimer has not been observed thus far. In order to get an idea which transitions can possibly be observed, in Table 2 we report the frequencies of the

Table 2
Frequencies (in cm^{-1}) and line strengths (in a.u.) of far-infrared transitions from the 10 lowest $J = 0$ states

i	f	$\Delta E(i \to f)$	$S(i \to f)$
1	2	19.33	0.0782
1	3	130.30	0.0616
1	6	263.80	0.0019
1	8	292.31	0.0010
1	9	327.72	0.0002
2	4	120.11	0.0054
2	5	157.69	0.0651
2	7	261.91	0.0000
2	10	372.53	0.0001
3	4	9.14	0.0890
3	5	46.72	0.0330
3	7	150.94	0.0926
3	10	261.56	0.0029
4	6	124.36	0.0016
4	8	152.87	0.0534
4	9	188.28	0.0108
5	6	86.78	0.0013
5	8	115.29	0.0151
5	9	150.70	0.1342
6	7	17.44	0.0140
6	10	128.06	0.0013
7	8	11.07	0.0674
7	9	46.48	0.0499
8	10	99.55	0.0151
9	10	64.14	0.0064

individual transitions from the lowest levels of $(H_2O)_2HCl$ and the corresponding vibrational line strengths. The latter quantity can be used to obtain line strengths of the individual rovibrational transitions when multiplied with a suitable Hönl-London factor. An inspection of Table 2 shows that several transitions in the frequency range ≈ 10–$160\ cm^{-1}$ should appear in the far-infrared with an appreciable intensity. It is interesting to note that the line strengths reported in Table 2 are dominated by the *a* component of the dipole function. This suggests that the a-type transitions will be the most intense in the far-infrared spectrum.

We wish to end this section by saying that while this work was about to be completed we learned that calculations of the $J = 0$ levels and of the Coriolis interaction for the three lowest states with $J = 1$ and for the five lowest states with $J = 2$ have been performed by the Nijmegen group of theoretical chemistry [35]. Wormer et al. [35] applied a potential energy surface from supermolecule coupled-cluster calculations including single, double, and non-iterative triple excitations. Their results are in a qualitative agreement with the present results, but some quantitative differences in the tunneling splittings can be observed. Comparison with future experiments will allow to discriminate between the two sets of calculations.

4. Conclusions

We obtained an ab initio SAPT potential for the torsional motions of the free hydrogen atoms in the $(H_2O)_2HCl$ trimer, and computed the VRT levels of the complex for $J = 0$ and $J = 1$. Our results show that the tunneling splittings that are dipole allowed are in the frequency range 10–$100\ cm^{-1}$, and have appreciable vibrational line strengths. Thus, they should be observed in a far-infrared experiment.

As far as the theory is concerned, we have shown that the three-body forces strongly affect the computed tunneling splittings. Thus, any theoretical calculation aiming to explain the spectroscopic features of the $(H_2O)_2HCl$ trimer should take into account the non-additive interactions.

Acknowledgements

We would like to thank Professor Bogumił Jeziorski for reading the manuscript and for useful comments. We also thank Jacek Kłos for his assistance in the fitting and in the preparation of figures.

References

[1] D.R. Handon, A.R. Ravishankara, J. Phys. Chem. 96 (1992) 2682.
[2] L.T. Chu, M.T. Leu, L.F. Keyser, J. Phys. Chem. 97 (1993) 12798.
[3] M.R.S. McCoustra, A.B. Horn, Chem. Soc. Rev. 23 (1994) 195.
[4] G.-J. Kroes, D.C. Clary, Geophys. Res. Lett. 19 (1992) 1355.
[5] G.-J. Kroes, D.C. Clary, J. Phys. Chem. 96 (1992) 7079.
[6] L. Wang, D.C. Clary, J. Chem. Phys. 104 (1996) 5663.
[7] A. Milet, C. Struniewicz, R. Moszynski, P.E.S. Wormer, J. Chem. Phys. 115 (2001) 345.
[8] A.C. Legon, L.C. Willoughby, Chem. Phys. Lett. 95 (1983) 449.
[9] Z. Kisiel, B.A. Pietrewicz, P.W. Fowler, A.C. Legon, E. Steiner, J. Phys. Chem. A 104 (2000) 6970.
[10] Z. Kisiel, E. Białkowska-Jaworska, L. Pszczółkowski, A. Milet, C. Struniewicz, R. Moszynski, J. Sadlej, J. Chem. Phys. 112 (2000) 5767.
[11] Z. Kisiel, J. Kosarzewski, B.A. Pietrewicz, L. Pszczolkowski, Chem. Phys. Lett. 325 (2000) 523.
[12] M.J. Packer, D.C. Clary, J. Phys. Chem. 99 (1995) 14323.
[13] A. Milet, C. Struniewicz, R. Moszynski, J. Sadlej, Z. Kisiel, E. Białkowska-Jaworska, L. Pszczółkowski, Chem. Phys. in press.
[14] A. Milet, C. Struniewicz, P.E.S. Wormer, R. Moszynski, Theor. Chem. Acc. 104 (2000) 195.
[15] K. Szalewicz, B. Jeziorski, Mol. Phys. 38 (1979) 191.
[16] R. Moszynski, B. Jeziorski, A. Ratkiewicz, S. Rybak, J. Chem. Phys. 99 (1993) 8856.
[17] R. Moszynski, B. Jeziorski, K. Szalewicz, J. Chem. Phys. 100 (1994) 1312.
[18] R. Moszynski, B. Jeziorski, S. Rybak, K. Szalewicz, H.L. Williams, J. Chem. Phys. 100 (1994) 5080.
[19] R. Moszynski, S.M. Cybulski, G. Chalasinski, J. Chem. Phys. 100 (1994) 4998.
[20] S. Rybak, B. Jeziorski, K. Szalewicz, J. Chem. Phys. 95 (1991) 6576.
[21] G. Chalasinski, B. Jeziorski, Theor. Chim. Acta 46 (1977) 277.
[22] M. Jeziorska, B. Jeziorski, J. Cizek, Int. J. Quantum Chem. 32 (1987) 149.
[23] R. Moszynski, T.G.A. Heijmen, B. Jeziorski, Mol. Phys. 88 (1996) 741.
[24] B. Jeziorski, R. Moszynski, K. Szalewicz, Chem. Rev. 94 (1994) 1887.

[25] B. Jeziorski, R. Moszynski, A. Ratkiewicz, S. Rybak, K. Szalewicz, H.L. Williams, SAPT: A program for many-body symmetry-adapted perturbation theory calculations of intermolecular interactions, in: E. Clementi (Ed.), Methods and Techniques in Computational Chemistry: METECC-94, vol. B Medium Size Systems, STEF, Cagliari, 1993, p. 79.
[26] R. Moszynski, P.E.S. Wormer, B. Jeziorski, A. van der Avoird, J. Chem. Phys. 103 (1995) 8058.
[27] R. Moszynski, P.E.S. Wormer, T.G.A. Heijmen, A. van der Avoird, J. Chem. Phys. 108 (1998) 579.
[28] A. Milet, R. Moszynski, P.E.S. Wormer, A. van der Avoird, J. Phys. Chem. A 103 (1999) 6811.
[29] P.E.S. Wormer, R. Moszynski, SAPT3 package, Nijmegen, 1996.
[30] P.R. Bunker, Molecular Symmetry and Spectroscopy, Academic Press, New York, 1979.
[31] M. Geleijns, A. van der Avoird, J. Chem. Phys. 110 (1999) 823.
[32] R.A. Kendall, T.H. Dunning Jr., R.J. Harrison, J. Chem. Phys. 96 (1992) 6769.
[33] P.E.S. Wormer, private communication.
[34] D.T. Colbert, W.H. Miller, J. Chem. Phys. 96 (1992) 1982.
[35] P.E.S. Wormer, G.C. Groenenboom, A. van der Avoird, to be published.